ISSN 1225-8024(Print)
ISSN 2288-8403(Online)

한국표면공학회지
J. Korean Inst. Surf. Eng.
Vol. 49, No. 2, 2016.
http://dx.doi.org/10.5695/JKISE.2016.49.2.147

<연구논문>

Corrosion of Fe-9%Cr-1%Mo Steel at 600 and 700°C in N_2/(0.5, 2.5)%H_2S-mixed Gas

Dong Bok Lee, Muhammad Ali Abro, Poonam Yadav, Sang Hwan Bak, Yuke Shi, Min Jung Kim*

School of Advanced Materials Science and Engineering, Sungkyunkwan University, Suwon 16419, Korea

(Received March 29, 2016 ; accepted April 12, 2016)

Abstract

The T91 steel (Fe-9%Cr-1%Mo) was corroded at 600 and 700°C for 5 - 70 h in the N_2/(0.5, 2.5)%H_2S-mixed gas at one atm. It was corroded fast, forming the outer FeS layer and the inner (FeS, $FeCr_2O_4$)-mixed layer. The formation of the outer FeS layer facilitated the oxidation of Cr to $FeCr_2O_4$ in the inner layer. Since the nonprotective FeS scale was present over the whole scale, T91 steel displayed poor corrosion resistance.

Keywords : T91 steel, Corrosion, Sulfidation, Oxidation, H_2S gas

1. Introduction

One of the main problems in oil refinery, carbo-chemistry, petrochemical units, carbon gasification, and energy generation in thermal power plants is the high-temperature corrosion occurring by the H_2S gas, which limits the operating temperature and the process efficiency [1-3]. The H_2S gas, which is produced as the by-product during processing, dissociates into sulfur and hydrogen, and reacts with the steel according to the reaction; $H_2S+Fe \rightarrow FeS+H_2$ [4,5]. Generally, sulfides are highly nonstoichiometric, and ionic diffusion in sulfides is hence faster than that in the corresponding oxides [6,7]. Sulfidation is therefore a quite serious problem. Not only sulfur but also hydrogen significantly decreases the corrosion resistance and mechanical properties of the steel through hydrogen embrittlement and hydrogen dissolution in the matrix and the scale [4,5].

In this study, ASTM T91 steel was corroded at 600 and 700°C for up to 70 h in N_2/(0.5, 2.5)%H_2S-mixed gas in order to understand its corrosion behavior in the H_2S-mixed gas. The T91 steel, containing 9Cr–1Mo (in wt%) with small additions of Mn, Si, V and Nb, has been used as structural components such as heat exchangers, boilers and pipes, because of its high temperature strength, creep resistance, high thermal fatigue life, good thermal conductivity, weldability, and resistance to graphitisation. Previously, the high-temperature corrosion of T91 steel under various corrosion conditions was extensively studied as follows. The oxidation in air, oxygen, and steam at 1 atm led to the formation of protective Cr_2O_3-rich scales, together with iron oxides [8]. The oxidation under high steam temperature and pressure in pressurised water reactors resulted in the formation of FeO and Fe_2O_3 at the gas/oxide interface, and Cr_2O_3 next to the oxide/metal interface [9]. When oxidized in Ar/(0.69 atm H_2O)-mixed steam at 575-650°C, T91 steel oxidized parabolically, developing triple-layered oxide layers that consisted of $(Fe,Cr)_3O_4$, Fe_3O_4, and Fe_2O_3 from the metal to the oxide/gas interface [10]. The corrosion of T91 steel in H_2/H_2S-mixed gas at 575-650°C led to the formation of (FeS, $FeCr_2S_4$)-sulfide scales, which tended to crack and

*Corresponding Author:Min Jung Kim
School of Advanced Materials Science and Engineering, Sungkyunkwan University
Tel: +82-31-290-7379 ; Fax: +82-31-290- 7410
E-mail: abc1219@skku.edu

spall off during cooling [11]. Further study on the effect of H_2S gas on corrosion is still needed, because the industrially important H_2S gas is particularly destructive owing to the formation of the nonprotective metal sulfide scales and the hydrogen dissolution [12]. The purpose of this study is to investigate the high-temperature corrosion behavior of T91 steel in N_2/H_2S-mixed gas.

2. Experimental Details

The T91 steel plate with a nominal composition of Fe-9Cr-1Mo-0.45Mn-0.4Si-0.2V-0.08Nb-0.1C in wt% was cut into a size of 2x10x15 mm^3, ground up to a 1000-grit finish with SiC paper, ultrasonically cleaned in acetone and alcohol, and corroded at 600 and 700 °C for 5-70 h in N_2/(0.5, 2.5)%H_2S-mixed gas at 1 atm. The corrosion tests were performed by suspending each sample with a Pt wire, and heating inside the vertical tube furnace. The employed N_2 gas was 99.999% pure, and H_2S gas was 99.5% pure. Since the H_2S gas was so corrosive, the thermogravimetric analyzer could not be used and the samples were corroded inside the quartz reaction tube. The corroded samples were characterized by a scanning electron microscope (SEM), an X-ray diffractometer (XRD) with Cu-Kα radiation, and an electron probe micro-analyzer (EPMA).

3. Results and Discussion

Figure 1 shows the corrosion kinetics of T91 steel in N_2/(0.5, 2.5)%H_2S gas. Weight gains were measured using a microbalance before and after each corrosion test, excluding the spontaneously spalled scale. All the scales that formed in this study were highly susceptible to spallation owing to the corrosion in H_2S. Hence, Fig. 1 is considered to show the under-estimated corrosion rates due to the inevitable scale spallation for all the samples. Nonetheless, the general corrosion trend can be outlined as follows. Weight gains increased with an increase in the temperature and the H_2S gas concentration. Particularly large weight gains were measured for the sample corroded at 700°C in N_2/2.5%H_2S gas. All the samples corroded almost linearly, indicating poor corrosion resistance. Local cracking and partial spallation of scales, together with void formation in the formed scales, were always unavoidable. It was however noted that T91 steel displayed good oxidation resistance in oxidizing atmospheres owing

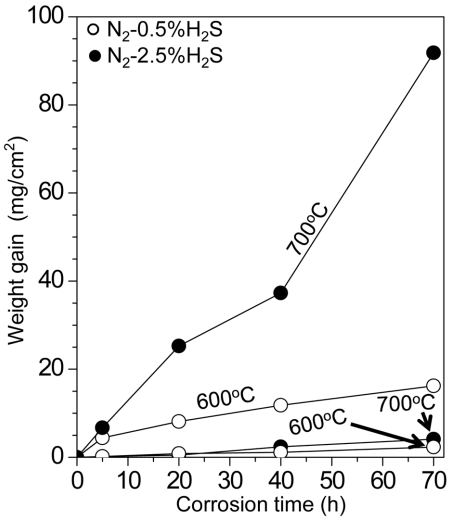

Fig. 1. Weight gain versus corrosion time curves of T91 steel at 600 and 700°C in N_2/(0.5, 2.5)%H_2S-mixed gas.

to the formation of the Cr_2O_3-rich scales [8]. The oxidation-resistant T91 steel sulfidized rapidly with large weight gains in H_2/H_2S-mixed gas [11].

The corrosion of T91 steel at 600 and 700 °C for 5 - 70 h in N_2/(0.5, 2.5)%H_2S gas always led to the formation of the outer FeS scale and the inner (FeS, $FeCr_2O_4$)-mixed scale, as typically shown in Fig. 2. The outer FeS scale was particularly nonadherent, and easily spalled off during corrosion and handling after corrosion. The spalled scale was collected, pulverized manually, X-rayed, and found to be composed of FeS (Fig. 2(a)). The underlying, retained inner scale was X-rayed, and found to be composed of FeS and $FeCr_2O_4$ (Fig. 2(b)). Here, the α-Fe matrix phase was also detected. It is seen that T91 steel reacted with the H_2S gas to form FeS according to the reaction; $Fe(s)+H_2S(g) \rightarrow FeS(s)+H_2(g)$. The released hydrogen would dissolve in the sample. Since FeS has a very high concentration of cation vacancies, it grew fast to form the outer scale through the outward diffusion of Fe^{2+} ions [13]. The formation of the outer FeS scale decreased the sulfur potential and depleted Fe in the inner scale, resulting in the formation of the inner ($FeCr_2O_4$, FeS)-mixed scale. The oxygen source for the formation of the $FeCr_2O_4$ spinel was the impurity oxygen in N_2/(0.5, 2.5)%H_2S-mixed gas. When Fe-(0.35-74) at.% Cr alloys sulfidized at 700 - 1000°C under atmospheric S_2 gas, the sulfidation ocurred several orders magnitude faster than the oxidation, and multiphase scales that consisted of FeS, $FeFe_{2-x}Cr_xS_4$, Cr_2S_3, and $FeCr_2S_4$ formed, depending on the Cr content [7]. The absence

Table 1. Standard free energies of formation (kJ) [14,15] and the Pilling-Bedworth ratios of sulfides and oxides [16-19].

reaction	ΔG^{o} (kJ) at 600°C	ΔG^{o} (kJ) at 700°C	P-B ratio (%)
$2Fe(s)+S_2 \rightarrow 2FeS(s)$	-207.4 [14]	-198.4 [14]	261 [16]
$2Fe(s)+O_2 \rightarrow 2FeO(s)$	-415 [14]	-402.2 [14]	1.78 [17]
$4/3\ Cr(s)+S_2 \rightarrow 2/3\ Cr_2S_3(s)$	-219.2 [15]	-204.2 [15]	-
$4/3\ Cr(s)+O_2 \rightarrow 2/3\ Cr_2O_3(s)$	-605.6 [14]	-588.7 [14]	2.02 [17]
$W(s)+S_2 \rightarrow WS_2\ (s)$	-218.2 [14]	-202.7 [14]	3.47 [18]
$W(s)+O_2 \rightarrow WO_2\ (s)$	-429.5 [14]	-412 [14]	1.87 [17]
$2Mn(s)+S_2 \rightarrow 2MnS(s)$	-439.2 [14]	-428.9 [14]	2.84
$2Mn(s)+O_2 \rightarrow 2MnO(s)$	-642.1 [14]	-627.6 [14]	1.75 [19]
$Si(s)+S_2 \rightarrow SiS_2(s)$	-201.9 [14]	-190.4 [14]	3.79
$Si(s)+O_2 \rightarrow SiO_2(s)$	-752.5 [14]	-735 [14]	2.15 [17]

of Cr-containing sulfides in this study was attributed to the low sulfur pressure and high oxygen pressure when compared to the corrosion condition employed in ref. [7] (viz. atmospheric S_2 gas).

Table 1 lists the standard free energies of formation [14,15] and the Pilling-Bedworth ratios of sulfides and oxides, which can be formed in this study [16-19]. In the standard state, the thermodynamic stability of the sulfides increases in the order of SiS_2, FeS, WS_2, Cr_2S_3, and MnS, and that of the oxides increases in the order of FeO, WO_2, Cr_2O_3, MnO, and SiO_2. All the oxides are thermodynamically more stable than their corresponding sulfides. In this study, FeS was the major scale because Fe was the major element and there was enough sulfur available in N_2/(0.5, 2.5)%H_2S gas. Since Cr_2O_3 is more stable than Cr_2S_3, FeS, and FeO, it formed and became the more stable $FeCr_2O_4$ spinel according to the equation; $Cr_2O_3(s)+FeO(s) \rightarrow FeCr_2O_4(s)$. Neither oxides nor sulfides of Si, Mn and W were not detected in Fig. 2 due to their dissolution in $FeCr_2O_4$ or FeS. Table 1 also shows that large volume expansion occurs during scaling, which generates the large growth stress in the scale. The volume expansion and the hydrogen dissolution are responsible for the poor adherence of the formed scales. The formation of nonprotective FeS and less protective $FeCr_2S_4$, along with the hydrogen dissolution, are the main reason for the poor corrosion resistance of T91 steel.

Fig. 1 indicated that the scaling rate increased with the increment of the H_2S gas concentration. The effect of the H_2S gas concentration on the growth rate of the major scale, FeS, may be explained as follows. The defect structure of FeS is the cation deficient $Fe_{1-x}S$ [13]. This is the p-type semiconductor, whose defect equation is given in eq. (1).

$$\frac{1}{2}S_2 = S_s + 2h + V_{Fe}'' \quad (1)$$

where S_s, $h^{\cdot}$ and V_{Fe}'' mean S atom on S site, electron hole in the valance band, and vacancy on Fe site with -2 charge relative to the normal site occupation, respectively. The equilibrium constant for eq. (1) may be written in terms of concentrations $C_{h\cdot}$ and $C_{V_{Fe}''}$ as in eq. (2).

$$C_{h\cdot}^2 \cdot C_{V_{Fe}''} = K_{(1)} p_{S_2}^{1/2} \quad (2)$$

For electrical neutrality, $C_{h\cdot} = 2C_{V_{Fe}''}$, and thus the eq. (3) is obtained:

$$C_{V_{Fe}''} = \text{const.} p_{S_2}^{1/6} \quad (3)$$

Hence, the diffusivity of Fe^{2+} ions through the divalent cation vacancy is expected to vary proportionally to the concentration of V_{Fe}'' and so with the sixth root of the sulfur partial pressure. Hence, the increment of the H_2S gas concentration led to the increment of growth rate of FeS or more weight gains, as shown in Fig. 1.

Figure 3 shows the EPMA results on the scale formed on T91 steel after corrosion in N_2-0.5%H_2S gas at 700°C for 70 h. The ~35 μm-thick outer scale was detached off from the ~20 μm-thick inner scale (Fig. 3(a)). The concentration profiles of sulfur and oxygen shown in Fig. 3(b) were consistent with the XRD result that indicated the formation of the outer FeS scale and the inner (FeS, $FeCr_2O_4$)-mixed scale. Voids formed in the scale owing to the anisotropic volume expansion during scaling (Table 1) and the outward diffusion of Fe^{2+} ions to form the outer FeS scale. The mismatch in the thermal expansion coefficients among FeS, $FeCr_2O_4$, and matrix as well as the hydrogen dissolution induce cracks in the

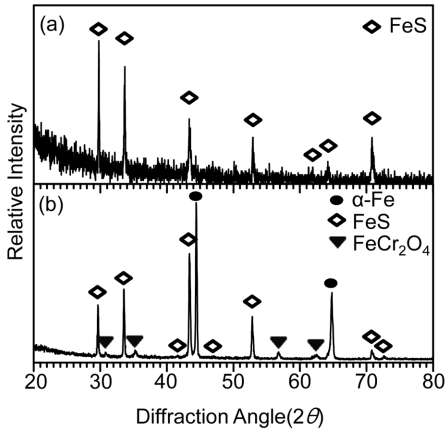

Fig. 2. XRD patterns of T91 steel after corrosion at 700°C for 20 h in N_2-2.5%H_2S gas. (a) outer scale, (b) inner scale.

scale. Voids and cracks would facilitate the detachment of the outer scale. Sulfur and oxygen can diffuse inward easily through voids and cracks. Fig. 3(b) indicates that Mo and Mn were dissolved not only in the outer FeS scale but also in the inner (FeS, $FeCr_2O_4$)-mixed scale, while Cr and Si were dissolved mainly in the inner (FeS, $FeCr_2O_4$)-mixed scale.

Figure 4 shows the EPMA results on the scale formed on T91 steel after corrosion in N_2-2.5%H_2S gas at 600°C for 40 h. It is noted that the EPMA analysis on the sample corroded in N_2-2.5%H_2S gas at 700°C for 70 h (*see* Fig. 3 corrosion condition) was impossible because the scale was too fragile. Fig. 4(a) shows ~50 μm-thick outer FeS scale and ~30 μm-thick inner (FeS, $FeCr_2O_4$)-mixed scale. In the epoxy, fragments of the outwardly growing FeS scale were embedded. Numerous voids aligned at the interface of the outer/inner scale, which would facilitate the detachment of the outer FeS scale. The outer FeS scale was not yet detached off. In Fig. 4(b), Mo and Mn were dissolved not only in the outer FeS scale but also in the inner (FeS, $FeCr_2O_4$)-mixed scale, while Cr was dissolved only in the inner (FeS, $FeCr_2O_4$)-mixed scale, as Mo, Mn, and Cr did in Fig. 3(b). However, Si was present not only in the inner mixed scale but also in the outer FeS scale in Fig. 4(b), although Si was mainly present in the inner mixed scale in Fig. 3(b). In Fig. 4, Mo, Mn, and Si diffused outwardly, together with Fe, to form the outer FeS scale. Such difference in the elemental distribution in the scale originated from the different diffusivity, concentration, solubility, and thermodynamic activity of each element.

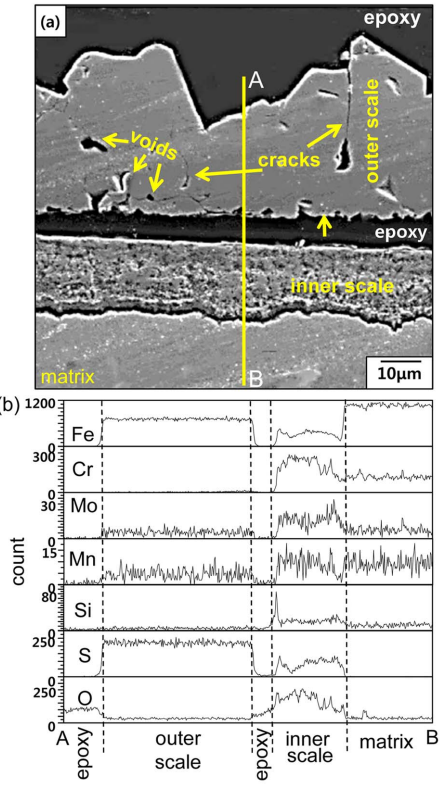

Fig. 3. EPMA analysis on the scale formed on T91 steel after corrosion in N_2-0.5%H_2S gas at 700°C for 70 h. (a) cross-sectional image, (b) line profiles along A-B.

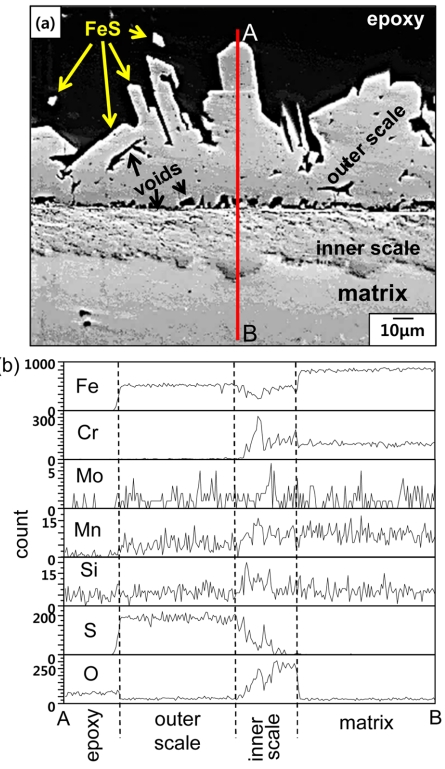

Fig. 4. EPMA analysis on the scale formed on T91 steel after corrosion in N_2-2.5%H_2S gas at 600°C for 40 h. (a) cross-sectional backscattered electron image, (b) line profiles along A-B.

4. Conclusions

T91 steel was corroded at 600 and 700°C for up to 70 h in N_2/(05, 2.5)%H_2S gas at 1 atm. The corrosion occurred almost linearly because H_2S formed the nonprotective FeS scale, together with $FeCr_2O_4$, and the dissolution of hydrogen in the scale occurred. The outward diffusion of Fe, and Mn led to the formation of the outer, nonadherent FeS scale dissolved with Mn. Cr and Si were enriched in the inner (FeS, $FeCr_2O_4$)-mixed scale. During corrosion, FeS kept growing through the outward diffusion of Fe^{2+} ions. The increment of the H_2S gas concentration thickened the scales. T91 steel was nonprotective, and formed mechanically weak scales in the H_2S environments.

Acknowledgments

This work was supported by the Human Resource Development Program (No. 20134030200360) of the Korea Institute of Energy Technology Evaluation and Planning (KETEP) grant funded by the Korea government Ministry of Trade, Industry and Energy.

References

[1] G. Y. Lai, High-Temperature Corrosion and Materials Applications, ASM International, USA (1990) 201-234.
[2] N. J Simms, J. F Norton, T. M. Lowe, Alloy corrosion in a coal gasification system, J. Phys. IV, 3 (1993) 807-816.
[3] R. John, Shreir's Corrosion, vol. 1, 4th ed., (eds. R. A. Cottis, M. J. Graham, R. Lindsay, S. B. Lyon, J. A. Richardson, J. D. Scantlebury, and F. H. Stott), Elsevier, UK (2010) 240-271.
[4] N. Birks, G. H. Meier, F. S. Pettit, Introduction to the High Temperature Oxidation of Metals, 2nd ed., Cambridge University Press, USA (2006) 163-168.
[5] D. J. Young, High Temperature Oxidation and Corrosion of Metals, T. Burstein, 1st ed., Elsevier, UK (2008) 361-396.
[6] S. Mrowec, K. Przybylski, Transport properties of sulfide scales and sulfidation of metals and alloys, Oxid. Met, 23 (1985) 107-139.
[7] S. Mrowec, T. Walec, T. Werber, High-temperature sulfur corrosion of iron-chromium alloys, Oxid. Met., 1 (1969) 93-120.
[8] A. S. Khanna, P. Rodriguez, J. B. Gnanamoorthy, Oxidation kinetics, breakaway oxidation, and inversion phenomenon in 9Cr-1Mo steels, Oxid. Met., 26 (1986) 171-200.
[9] A. P. Greeff, C. W. Louw, H. C. Swart, The oxidation of industrial FeCrMo steel, Corros. Sci., 42 (2000) 1725-1740.
[10] D. Laverde, T. Gomez-Acebo, F. Castro, Continuous and cyclic oxidation of T91 ferritic steel under steam, Corros. Sci., 46 (2004) 613-631.
[11] F. Gesmundo, F. Viani, W. Znamirowski, K. Godlewski, F. Bregani, The Corrosion of iron and of three commercial steels in H_2-H_2S and in H_2-H_2S-CO_2 gas mixtures at 400-700°C, Mater. Corros., 43 (1992) 83-95.
[12] M. A. Abro, D. B. Lee, Aluminizing and corrosion of carbon steels in N_2-0.5%H_2S gas at 650-850°C, J. Kor. Inst. Surf. Eng., 48 (2015) 110-114.
[13] M. Danielewski, S. Mrowec, A. Stołosa, Sulfidation of iron at high temperatures and diffusion kinetics in ferrous sulfide, Oxid. Met., 17 (1982) 77-97.
[14] I. Barin, Thermochemical Data of Pure Substances, VCH, Germany (1989).
[15] L. B. Pankratz, A. D. Mah, S. W. Watson, Thermodynamic properties of sulfides, U.S. Bur. Min. Bull., 689 (1987) 472.
[16] M. J. Kim, D. B. Lee, Corrosion of Fe-(4.8, 9.2, 14.3) wt% Al alloys at 700 and 800°C in N_2/H_2O/H_2S gases, Met. Mater. Int., 19 (2013) 975-982.
[17] A. S. Khanna, Introduction to High Temperature Oxidation and Corrosion, ASM International, USA (2002) 204.
[18] Gmelin Institute for Inorganic Chemistry, Gmelin Handbook of Inorganic Chemistry, Vol. A7, 8th ed., Springer, Germany (1987).
[19] E. McCafferty, Introduction to Corrosion Science, Springer, USA (2010) 236.